



Preparation of nano-sized magnetic particles from spent pickling liquors by ultrasonic-assisted chemical co-precipitation

Bing Tang^{a,*}, Liangjun Yuan^a, Taihong Shi^b, Linfeng Yu^a, Youchun Zhu^a

^a Faculty of Environmental Science and Engineering, Guangdong University of Technology, Guangzhou 510006, PR China

^b Faculty of Environmental Science and Engineering, Sun Yat-sen University, Guangzhou 510275, PR China

ARTICLE INFO

Article history:

Received 31 December 2007

Received in revised form 20 April 2008

Accepted 18 July 2008

Available online 29 July 2008

Keywords:

Spent pickling liquors

Magnetic materials

Nano-sized particles

Ultrasonic-assisted process

ABSTRACT

The aim of this study is to develop a new method for the preparation of high-value, environmentally friendly products from spent pickling liquors. An ultrasound treatment was introduced into a chemical co-precipitation process to control the size of the particles produced. The particles were characterized by X-ray powder diffraction and transmission electron microscopy. The magnetic parameter was measured with a magnetic property measurement system. The product consisted of ferrous ferrite (Fe_3O_4) nano-sized cubic particles with a high level of crystallinity that exhibited super-paramagnetism.

© 2008 Elsevier B.V. All rights reserved.

1. Introduction

Spent pickling liquors containing high concentrations of iron and residual acid are hazardous waste products of the surface treatment of steel. Generally, the liquors are neutralized and the metals precipitated, followed by discharge. However, this procedure generates large amounts of unstable sludge, which need to be disposed of to avoid secondary pollution. Due to the high concentration of iron, spent pickling liquors may represent a cheap source of raw material for the production of many kinds of chemicals. In the past decade, some new approaches have been investigated for the treatment of spent pickling liquors, including anion-exchange/membrane electrowinning [1], microwave-hydrothermal process [2], electro-dialysis [3], membrane distillation [4], selective precipitation [5,6], solvent extraction [7], and use in the production of concrete [8]. These investigations have led to the disposal of spent pickling liquor without any toxic effluent in some cases, but most of these processes lead to the production of iron salts, iron oxides or reuse of the acid, which may suffer some market restrictions. Ciminelli et al. [2] has emphasized the importance of producing a more valuable product from spent pickling liquors with regard to both environmental considerations and cost. So, there is a need for a simple treatment method that will yield high-value products from spent pickling liquors.

Ferrous ferrite (Fe_3O_4) is a traditional magnetic material that has found many applications in magnetic storage media, solar energy transformation, electronics, and catalysis. When it is dispersed as nano-scale particles, the physical and chemical properties are quite different from those of the bulk material, and often exhibits desirable properties, such as high-field saturation and extra anisotropy contributions [9], suggesting physical applications and uses in biomedicine. For example, in recent years, there have been many reports of the applications of nano-sized Fe_3O_4 in magnetic resonance imaging (MRI) contrast agents [10], biosensor [11], and embolotherapy [12]. Although Fe_3O_4 has been synthesized through different approaches [13], the chemical co-precipitation process is the most common. However, in most cases, the particles formed are only just within the micrometer scale [14], and it is difficult to control the size distribution and scale in an ordinary chemical co-precipitation process [15]. The rapid progress of microelectronic technology and other fields of industry require continuous reduction of component size, stimulating the demand for synthesis of ultra-fine particles and functional materials.

Much attention has been paid to ultrasound/chemical (sono-chemical) methods for the production of nanomaterials [16]. The transmission of ultrasound in a liquid phase provides mixing conditions favorable for chemical reaction, and generates transient extreme temperature or high shear-rate through acoustic cavitations, which has a specific effect on a chemical reaction that is very suitable for the formation of nanoparticles. Several kinds of nanoparticles have been synthesized by this method [17–20]; for example, inorganic nanoparticles of Fe_2O_3 , CdS, Mn_3O_4 , and

* Corresponding author. Tel.: +86 20 39322296; fax: +86 20 38457257.
E-mail address: renyantang@163.com (B. Tang).

ZnS have properties ideally suited to catalysis, luminescence, high-density recording media, and non-linear optical devices, demonstrating the advantages of sonochemical methods in yielding smaller particles [21].

There are two main approaches to fabricate Fe₃O₄ nanoparticles: one is chemical co-precipitation [9,22], which always needs a surfactant to control the particle size and distribution and the other is sonochemistry [11,23,24], which always needs an expensive precursor as the source of iron. Generally, Fe₃O₄ nanoparticles produced by the sonochemical method are either amorphous or crystalline. The amorphous particles are always obtained by sonolyzing the volatile precursor inside the collapsing bubble, and the crystalline particles are obtained by the sonochemical reaction that occurs in the interfacial liquid region around the cavitation bubbles with non-volatile salts. In previous works, Kim et al. [10] compared the properties of Fe₃O₄ nanoparticles obtained by sonochemical and chemical co-precipitation methods with the same precursor, and found that the products of both methods had spinel magnetite crystal structure, but the magnetite nanoparticles produced by the sonochemical method had a higher level of crystallinity. Jiang et al. [9] obtained highly crystalline Fe₃O₄ nanoparticles by chemical co-precipitation, and found that the pivotal factor was the homogeneous pH condition in the process of forming the Fe₃O₄ nanoparticles. Ciminelli et al. [2] indicated that single-phase magnetite was obtained at pH 13 (110 °C for 5 min); otherwise, lower pH values and temperatures led to the production of other iron oxides. Kim et al. [25] discussed the importance of pH values in controlling the crystal size of Fe₃O₄.

Among the reports of the fabrication of Fe₃O₄ nanoparticles, the sonochemical and chemical co-precipitation methods both have relative advantages and disadvantages. Chemical co-precipitation is simple and cheap. The sonochemical method requires expensive organometallic compounds as precursors, but offers better control of the size and size distribution of particles. There have been few reports of the production of ferrite nanoparticles from spent pickling liquors, but Konishi et al. [26] and López et al. [27] have investigated the synthesis of complex ferrite (nickel ferrite and zinc ferrite) by microbial oxidization of Fe(II) to Fe(III) in dilute conditions.

An ultrasound-assisted chemical co-precipitation procedure may offer a promising method for the synthesis of nano-sized ferrite particles with spent pickling liquor as a precursor. In the present investigation, it was focused on the development of a new method to prepare high-value products from spent pickling liquors with advantages for the environment. Two related aspects were considered: (1) to investigate the possibility of producing magnetic nanoparticles from spent pickling liquors instead of expensive organometallic compounds in an ultrasonic process and (2) to characterize the products. We proposed a procedure of ultrasonic-assisted chemical co-precipitation, and characterized the products with X-ray powder diffraction (XRD) and transmission electron microscopy (TEM); the magnetic property was measured with a magnetic property measurement system (MPMS).

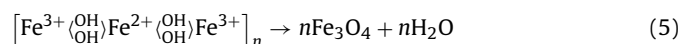
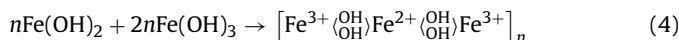
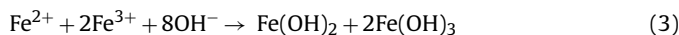
2. Basic mechanism

2.1. Formation of Fe₃O₄

In alkaline solutions, Fe(III) and Fe(II) precipitate spontaneously with a small solubility product constant. If there is only Fe(III) or Fe(II) in the solution, the precipitates are only the hydroxides of Fe(III) or Fe(II), which can be expressed as:



If these two kinds of ion are mixed in alkaline conditions, the hydroxides formed may be adsorbed mutually, produce a new kind of mixture that is highly unstable in normal conditions, and can be stripped of water in its molecular structure. That is the reaction of producing Fe₃O₄, which can be expressed as:



2.2. Particle growth and ultrasound function

Once a core of Fe₃O₄ crystal is formed, the liquid phase becomes a two-phase system and, because of the tremendous surface energy, small crystals tend to aggregate to form larger particles. The mechanism expressed by Eq. (5) indicates the formation process of the Fe₃O₄ core, which involves adsorption and dehydration of the hydroxides of Fe(II) and Fe(III). By this mechanism, the growth pattern is simply the aggregation of particles and, in most cases, the stability of particles can be expressed as:

$$W = (a + b) \int_{a+b}^{\infty} \exp \left[\frac{V(R)}{k_B T} \right] \frac{dR}{R^2} \quad (6)$$

where W is the stability factor of particles, a and b are the radius of the two particles, respectively, R is the distance between the two particles, and $V(R)$ is the function of potential energy of interaction, and k_B is Boltzmann's constant. When the distance between particles is decreased to a certain extent, short-range reactions (such as van der Waals forces) may lead to strong attraction between particles. Generally, in the process of reaction without any external disturbance around a crystal, the particles of Fe₃O₄ can approach each other and aggregate easily, growing gradually into larger particles that reach the micrometer scale or larger. So, it is important to maintain sufficient distance between particles for the stability of the multi-phase system.

The novel effects of ultrasound spreading through a liquid phase are regarded to arise from acoustic cavitations, which consist of the creation, growth and implosive collapse of gas vacuoles in solution. As a result of these effects, an alternating pressure field occurs within the bubbles during cavitation collapse [28], which leads to a transient high-temperature, high-pressure environment or high shear-rate in solution, and provides conditions suitable for forming crystal nuclei with a high-reaction rate. Abundant crystal cores formed instantaneously decrease the degree of oversaturation of solution, which restricts growth of the crystal core. At the same time, transient high temperature during sonication that arisen from ultrasonic cavitation and the large amounts of tiny bubbles produced on the surface of solid particles decrease the dangling bonds and defects on the surface of the nuclei, and the surface state of the nuclei becomes stable [29]. So, with the action of ultrasonic cavitation, a high shear-rate is maintained throughout the solution, and the distance between particles can be sustained by the bubbles until the end of the reaction. In addition, the shock-wave that arisen by acoustic cavitation leads to strong shearing and fragmentation into particles, disrupting the aggregation between particles and control the size and size distribution, the surface activity of particles may also be restrained [30].

The influence of shearing on the aggregation of particles can be expressed by the dimensionless Peclet number (Pe) as [31]:

$$Pe = 3\pi \eta_c \sigma^3 \frac{u}{4k_B T} \quad (7)$$

where η_c is the viscosity of the continuous phase, u is the shear rate, and k_B is Boltzmann's constant. If Pe is much larger than 1, the shear-rate has an important influence on the aggregation of particles.

When the frequency of ultrasound is >20 kHz, transient formation and collapse of bubbles around particles can break chemical bonds, and the fast kinetics does not permit the growth of nuclei, which effectively prevents aggregation of particles; the precipitates can occur only in a uniform state of ultra-fine particles, so the stability of the system can be retained for a relatively long time without the need for a surfactant [23].

3. Experimental details

3.1. Main parameters

As discussed above, it is necessary to sustain stable thermodynamic and kinetic conditions in the reaction system for fabricating nano-scale Fe_3O_4 ; the homogeneous pH value and intensive disturbance throughout the solution are especially important.

A homogeneous pH value in the solution is an imperative factor for controlling the chemical species and size distribution of the Fe_3O_4 particles synthesized. In the experiments of this study, the pH value in the reaction system was maintained at 13 by a sodium hydroxide buffer solution. The molar ratio of Fe(III)/Fe(II) was adjusted to 2:1 by adding a stoichiometric proportion of sodium perchlorate ($NaClO_4$) into spent pickling liquors for oxidizing Fe(II) to Fe(III) more rapidly than was possible by microbial oxidation. The temperature of the whole reactor was maintained at $75^\circ C$. An ultrasonic reactor provided continuous and homogeneous ultrasonic irradiation all over the solutions; the frequency was 40 kHz, and the intensity of the ultrasound was adjusted by altering the input voltage.

3.2. Reagents and instruments

3.2.1. Chemicals

Spent pickling liquors (pH 0.3–0.5, total iron 105.6 g/L, HCl 10.6 g/L, trace amounts of other heavy metals, e.g. Mn 16.7 mg/L and Cr 8.9 mg/L) from a steel surface treatment factory were passed through a filter (filled with plastic stuffings) to remove suspended solids (SS) before being used as feed solutions. All other chemicals were of reagent grade. Sodium perchlorate ($NaClO_4$), which was used to adjust the ratio of Fe(III) and Fe(II) by oxidizing Fe(II), and sodium hydroxide (NaOH) were from the Tianjin Chemical Agent Factory.

3.2.2. Instruments

An ultrasonic reactor (HN1006B, Huanan, Guangzhou) was used to provide the ultrasonic field. X-ray powder diffraction (Y-4Q, Aolong, DanDong) was used to analyze the phase and measure the average size of particles. The morphological characteristics of the particles were observed with transmission electron microscopy (H-7500, Hitachi, Tokyo), and the magnetic properties were measured by a magnetic property measurement system (XL-7, Quantum Design, San Diego). The pH value in the solution was measured by a pH meter (PHS-25, LIDA, Shanghai).

3.3. Experimental process

Continuous and homogeneous ultrasound was provided by an ultrasonic reactor, whose intensity was adjusted by controlling the input voltage. Spent pickling liquors with known molar ratios of Fe(III)/Fe(II) served as feed solutions. To maintain constant and homogeneous pH throughout the solution, the reactor was filled with alkaline buffer solution (pH 13) in advance, the feed solution was added dropwise after the ultrasonic reactor was started, and at the same time, a stoichiometric amount of sodium hydroxide solution was added to the reactor to minimize any variation of pH (see Fig. 1). After reaction for 20–30 min, the mixture was allowed to separate into solid and liquid by sedimentation. The liquid was returned to the ultrasonic reactor and the solid was washed with distilled water to remove all of the NaCl that had formed, and then dried at $75^\circ C$ to constant weight. The experimental process is illustrated in Fig. 1.

4. Results and discussion

4.1. Phase observation

After the reactor was started, an obvious ripple emerged instantly on the surface of the solution. When the feed solution was dropped into the reactor, it was quickly dispersed and mixed throughout the reactor contents. At the same time, Fe(III) and Fe(II) ions reacted with hydroxyl to form a mixed hydroxide, which was highly unstable and could be dehydrated at a certain temperature to produce Fe_3O_4 . With a disturbed environment in the reactor, Fe_3O_4 crystals could not grow to a large size, and because the strength of the disturbance around a particle was the same in every direction, the particles had a regular structure.

Some magnetic particles were obtained under these experimental conditions. Y4Q XRD was used for phase observation of the particles obtained, and the results were shown in Fig. 2.

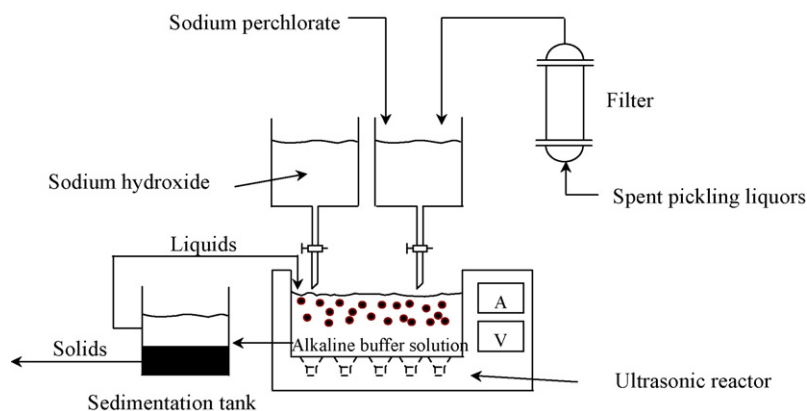


Fig. 1. Schematic diagram of the ultrasonic-assisted chemical co-precipitation process.

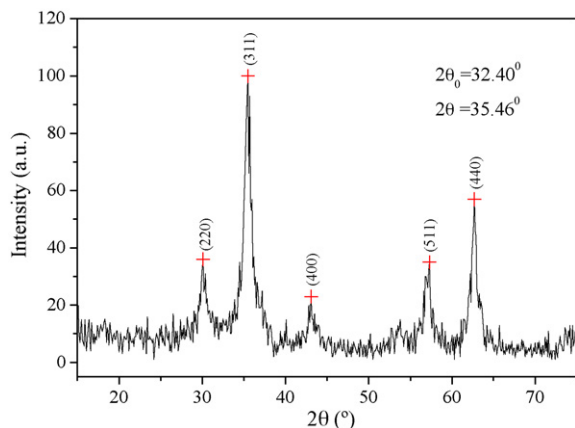


Fig. 2. XRD pattern of the obtained Fe_3O_4 nanoparticles.

Fig. 2 showed the XRD pattern of the synthesized particles, compared with the standard diffraction spectrum. The product was Fe_3O_4 crystal, and there was no other phase such as $\text{Fe}(\text{OH})_3$ or Fe_2O_3 , which were the usual co-products in chemical co-precipitation procedures. The sharpness of the peaks showed clearly that the synthesized Fe_3O_4 had a highly crystalline nature.

The special structure of Fe_3O_4 crystal could accommodate large number of ions in both octahedral and tetrahedral sites that offered an opportunity to engineer specific magnetic interactions in the crystal lattice by substituting or incorporating various transition metal cations into the crystal structure. According to this mechanism, other trace metal ions such as Mn or Cr were very easy to co-precipitate with Fe_3O_4 to form a kind of complex magnetite ferrite that was expressed with a general formula of $\text{MO}\cdot\text{Fe}_2\text{O}_3$. Because of very low concentration in feed solutions, almost all of these metal ions were stripped with the complex magnetite ferrite, and nearly left no metal ions in supernatant liquors [2]. Compared with the amount of Fe in magnetite ferrite, other trace metal ions occupied less sites in the structure of crystal, it had no impact to the structure of Fe_3O_4 crystal (see Fig. 2).

4.2. Particle size

The average size of particles was analyzed by X-ray powder diffraction, and evaluated from the Scherrer equation:

$$L = \frac{0.94\lambda}{B(2\theta)\cos\theta} \quad (8)$$

where L is the average diameter of the particles, λ is the wavelength of the incident X-ray, θ is the Bragg peak angle and corresponds to the angle of the (311) peak, $B(2\theta)$ is the full-width (in radians) subtended by the half-maximum intensity width of the powder peak, and 2θ is 35.46° (Fig. 2).

In order to investigate the shape of the synthesized particles, the average size was measured for each sample for three different apices, and for each apex, the average diameter of the particles were measured by XRD and calculated with Eq. (8). The data shown in Table 1 indicated a homogenous size of particles produced as shown in Fig. 1. The results in Table 1 suggested that the synthesized particles might be spherical or cubic.

In a sonochemical reaction, the morphology of products was totally determined by the precursors, if the precursors were volatile compound, the predominant reaction occurred in gas phase, which produced amorphous nanoparticles, but on the other hand, the precursors were non-volatile inorganic salts, the predominant reaction occurred in liquid phase which localized on a 200 nm-ring

surrounding the collapsing bubble [32] and produced nanocrystalline, this small reaction region also restricted the growth of the particles.

4.3. TEM measurement

The shape and size of the synthesized particles were observed by TEM (see Fig. 3). The results shown in Fig. 3 were quite in accord with the XRD data given in Table 1. In Fig. 3(a), most particles exhibited a cubic shape, and Fig. 3(b) showed that the particles were almost homogenous in size distribution.

The reactor used in our experiments equipped with equally installed ultrasonic transducers, which transformed electrical energy to ultrasonic vibration energy and transferred it to the solutions. The acoustic cavitation arisen by ultrasound produced large amount of tiny and homogenous bubbles that collapsed in less than a nanosecond, and formed an intense homogenous wave field, which provided a beneficial condition to obtain regular shaped particles with homogenous size distribution.

4.4. Magnetic property

The magnetic property of the nanoparticles was measured with an MPMS XL-7. The magnetic hysteresis curve in Fig. 4 with no hysteresis loop indicated that particles exhibited superparamagnetism. The saturation magnetization was 67.77 emu/g, and the remanence was 3.69 emu/g.

Table 1
Average size of the particles

Samples	No. of apex	Average diameter of particles (nm)
1	1	15.87
	2	14.24
	3	13.49
2	1	18.17
	2	16.52
	3	16.59
3	1	19.17
	2	18.77
	3	16.03
4	1	18.99
	2	13.82
	3	16.08
5	1	20.27
	2	22.14
	3	19.99
6	1	15.26
	2	14.39
	3	18.96
7	1	16.54
	2	14.40
	3	18.15
8	1	19.31
	2	16.53
	3	19.11
9	1	18.70
	2	16.56
	3	16.58
10	1	22.89
	2	19.12
	3	22.55

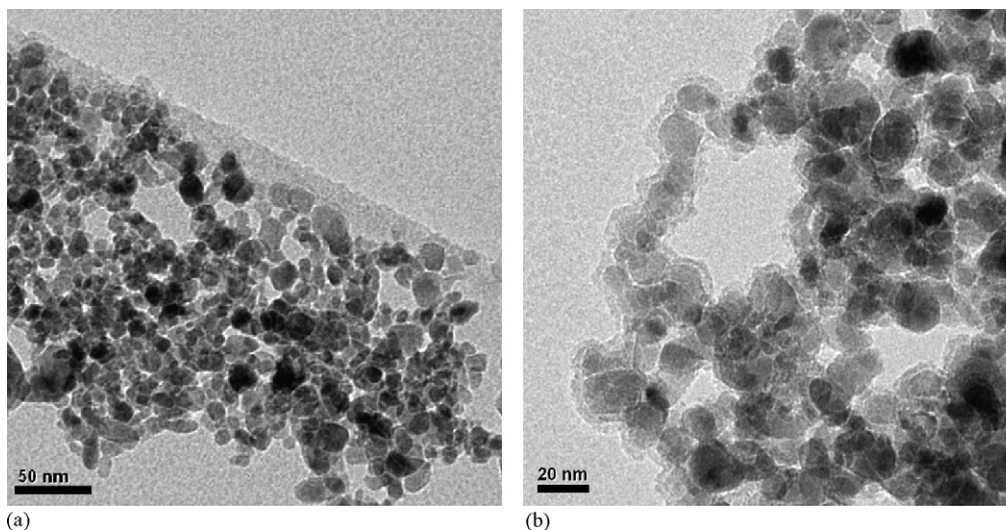


Fig. 3. TEM image of the obtained Fe_3O_4 nanoparticles: (a) Mag = 120.00K \times and (b) Mag = 200.00K \times .

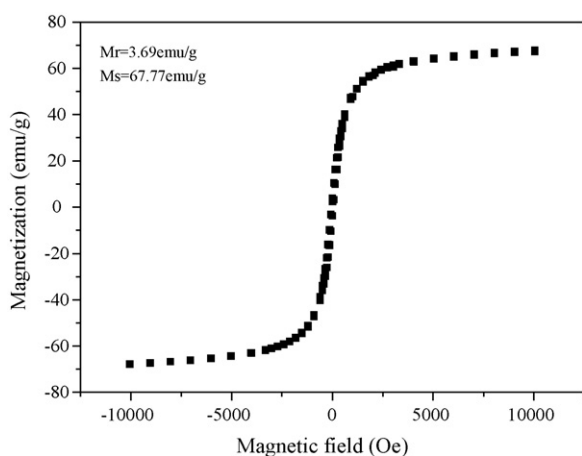


Fig. 4. Magnetic hysteresis curve of the prepared particles at 300 K.

Generally, a bulk ferromagnetic compound is multidomain in nature, the multidomain character reduces the total magnetization, but when the size of ferromagnetic compound is decreased below the critical size of single-domain particle, the magnetization of the ferromagnetic particles naturally align along the easy direction of magnetizations, which is the character of super-paramagnetism. From the reported literature [33,34], the critical size of a single-domain particle was demonstrated to be about 40–60 nm. The results shown in Fig. 4 also confirmed the resultant particles in our experiments were nanoparticles.

5. Conclusions

Nanoparticles of Fe_3O_4 were synthesized by ultrasonic-assisted chemical co-precipitation from spent pickling liquors from the steel surface treatment industry, instead of from expensive organometallic compounds. The cubic Fe_3O_4 particles of 13–23 nm diameter exhibited super-paramagnetic behavior and a high level of crystallinity, with homogenous size and shape distribution. The procedure proposed in our investigation needs no surfactant, and is easy to generalize because it is environmentally friendly, simple and cheap.

Acknowledgement

We are grateful for financial support from the Science and Technology Plan Program of Guangdong Province under grant number 2003A3030202.

References

- [1] G. Csicsovszki, T. Kekesi, T.I. Torok, Selective recovery of Zn and Fe from spent pickling solutions by the combination of anion exchange and membrane electrowinning techniques, *Hydrometallurgy* 77 (2005) 19–28.
- [2] V.S.T. Ciminelli, A. Dias, H.C. Braga, Simultaneous production of impurity-free water and magnetite from steel pickling liquors by microwave-hydrothermal processing, *Hydrometallurgy* 84 (2006) 37–42.
- [3] E. Paquay, A.M. Clarinval, A. Delvaux, M. Derez, H.D. Hurwitz, Applications of electrodialysis on acid pickling wastewater treatment, *Chem. Eng. J.* 79 (2000) 197–201.
- [4] M. Tomaszewska, M. Grypta, A.W. Morawski, Recovery of hydrochloric acid from metal pickling solutions by membrane distillation, *Sep. Purif. Technol.* 22–23 (2001) 591–600.
- [5] J. Dufour, L. López, C. Negro, R. Latorre, A. Formoso, F. Lopez-Mateos, Mathematical model of magnetite synthesis by oxidation of sulfuric pickling liquors from steelmaking, *Chem. Eng. Commun.* 189 (2002) 285–297.
- [6] F. Heras, J. Dufour, A. Lopez-Delgado, C. Negro, F. Lopez-Mateos, Feasibility study of metals recycling from nitric–hydro–fluoric waste pickle baths, *Environ. Eng. Sci.* 21 (2004) 583–590.
- [7] A. Agrawal, S. Kumari, B.C. Ray, K.K. Sahu, Extraction of acid and iron values from sulphate waste pickle liquor of a steel industry by solvent extraction route, *Hydrometallurgy* 88 (2007) 58–66.
- [8] A. Singhal, S. Prakash, V.K. Tewari, Trials on sludge of lime treated spent liquor of pickling unit for use in the cement concrete and its leaching characteristics, *Build. Environ.* 42 (2007) 196–202.
- [9] W.Q. Jiang, H.C. Yang, S.Y. Yang, H.E. Horng, J.C. Hung, Y.C. Chen, C.Y. Hong, Preparation and properties of superparamagnetic nanoparticles with narrow size distribution and biocompatible, *J. Magn. Magn. Mater.* 283 (2004) 210–214.
- [10] E.H. Kim, H.S. Lee, B.K. Kwak, B.K. Kim, Synthesis of ferrofluid with magnetic nanoparticles by sonochemical method for MRI contrast agent, *J. Magn. Magn. Mater.* 289 (2005) 328–330.
- [11] H.T. Chana, Y.Y. Doa, P.L. Huang, Preparation and properties of bio-compatible magnetic Fe_3O_4 nanoparticles, *J. Magn. Magn. Mater.* 304 (2006) e415–e417.
- [12] J. Liu, G.A. Flores, R.S. Sheng, In-vitro investigation of blood embolization in cancer treatment using magnetorheological fluids, *J. Magn. Magn. Mater.* 225 (2001) 209–217.
- [13] M. Ding, H.X. Zeng, Status and expectation of waste water containing heavy metal treatment with ferrite process, *J. Environ. Sci.* 13 (1992) 59–67.
- [14] W.S. Wang, L.X. Zheng, F.X. Gao, Investigation on the preparation of ferromagnetic fluid using spent steel pickle liquor in steel rolling, *Metals Mine* 1 (1994) 44–46.
- [15] Z.Q. Jia, Z.Z. Liu, Principle and characteristic of the process in preparing nanoparticle with the method of precipitation in liquid phase, *Chem. Eng.* 30 (2002) 38–41.
- [16] A. Gedanken, Using sonochemistry for the fabrication of nanomaterials, *Ultrason. Sonochem.* 11 (2004) 47–55.

- [17] C.S. Lee, J.S. Lee, S.T. Oh, Dispersion control of Fe_2O_3 nanoparticles using a mixed type mechanical and ultrasonic milling, *Mater. Lett.* 57 (2003) 2643–2646.
- [18] G.Z. Wang, W. Chen, C.H. Liang, Y.W. Wang, G.W. Meng, L.D. Zhang, Preparation and characterization of CdS nanoparticles by ultrasonic irradiation, *Inorg. Chem. Commun.* 4 (2001) 208–210.
- [19] I.K. Gopalakrishnan, N. Bagkar, R. Ganguly, S.K. Kulshreshtha, Synthesis of superparamagnetic Mn_3O_4 nanocrystallites by ultrasonic irradiation, *J. Cryst. Growth* 280 (2005) 436–441.
- [20] M. Behboudnia, M.H. Majlesara, B. Khanbabaee, Preparation of ZnS nanorods by ultrasonic waves, *Mater. Sci. Eng. B* 122 (2005) 160–163.
- [21] L.X. Yin, Y.Q. Wang, G.S. Pang, Y. Koltypin, A. Gedanken, Sonochemical synthesis of cerium oxide nanoparticles—effect of additives and quantum size effect, *J. Colloid Interf. Sci.* 246 (2002) 78–84.
- [22] L.M. Lacava, B.M. Lacava, R.B. Azevedo, Z.G.M. Lacava, N. Buske, A.L. Tronconi, P.C. Morais, Nanoparticle sizing: a comparative study using atomic force microscopy, transmission electron microscopy, and ferromagnetic resonance, *J. Magn. Magn. Mater.* 225 (2001) 79–83.
- [23] R. Vijayakumar, Y. Koltypin, I. Felner, A. Gedanken, Sonochemical synthesis and characterization of pure nanometer-sized Fe_3O_4 particles, *Mater. Sci. Eng. A* 286 (2000) 101–105.
- [24] R.A. Mukh-Qasem, A. Gedanken, Sonochemical synthesis of stable hydrosol of Fe_3O_4 nanoparticles, *J. Colloid Interf. Sci.* 284 (2005) 489–494.
- [25] D.K. Kim, Y. Zhang, W. Voit, K.V. Rao, M. Muhammed, Synthesis and characterization of surfactant-coated super-paramagnetic mono-dispersed iron oxide nano-particles, *J. Magn. Magn. Mater.* 225 (2001) 30–36.
- [26] T. Konishi, T. Nomura, K. Mizoe, A new synthesis route from spent sulfuric acid pickling solution to ferrite nanoparticles, *Hydrometallurgy* 74 (2004) 57–65.
- [27] F.A. López, A. López-Delgado, J.L. Martín de Vidales, E. Vila, Synthesis of nanocrystalline zinc ferrite powder from sulphuric pickling waste water, *J. Alloy Compd.* 265 (1998) 291–296.
- [28] K.S. Suslick, S.J. Doktycs, E.B. Flint, On the origin of sonoluminescence and sonochemistry, *Ultrasonics* 28 (1990) 280–290.
- [29] H. Wang, J.J. Zhu, J.M. Zhu, et al., Sonochemical method for the preparation of bismuth sulfide nanorods, *J. Phys. Chem. B* 106 (2002) 3848–3854.
- [30] J.C. Yu, Y.J. Guo, W. Ho, et al., Preparation of highly photocatalytic active nano-size TiO_2 particles via ultrasonic irradiation, *Chem. Commun.* 19 (2001) 1942–1948.
- [31] C.F. Zukoski, D.F. Rosenbaum, P.C. Zamora, Aggregation in precipitation reactions: stability of primary particles, *Trans. I Chem. E* 74A (1996) 723–731.
- [32] K.S. Suslick, D.A. Hammerton, R.E. Cline, The sonochemical hot spot, *J. Am. Chem. Soc.* 108 (1986) 5641–5642.
- [33] N.S. Gajbhiye, S. Prasad, G. Blaji, Experimental study of Hopkinson effect in single domain CoFe_2O_4 particles, *IEEE Trans. Magn.* 35 (1999) 2155–2161.
- [34] M. Kiyama, Particle growth of $\text{Co}_x\text{Fe}_{3-x}\text{O}_4$ with $x < 0.2$ by air oxidation of aqueous suspensions, *Bull. Inst. Chem. Res.* 60 (1982) 247–253.